Development of 325 MHz Single Spoke Resonators at Fermilab

G. Apollinari, I. V. Gonin, T. N. Khabiboulline, G. Lanfranco, A. Mukherjee, J. Ozelis, L. Ristori†, D. Sergatstkov, R. Wagner, R. Webber.

***Abstract*—The High Intensity Neutrino Source (HINS) project represents the current effort at Fermilab to produce an 8-GeV proton linac based on 400 independently phased superconducting cavities. Eighteen β=0.21 single spoke resonators, operating at 325 MHz, comprise the first stage of the linac cold section. In this paper we present the current status of the production and testing of the first two prototype cavities. This includes descriptions of the fabrication, frequency tuning, chemical polishing, high pressure rinse, and high-gradient cold tests.**

***Index Terms*— Accelerator cavities, niobium, superconducting device fabrication, superconducting device testing, superconducting cavity resonators.**

I. INTRODUCTION

FERMILAB is designing and building the front end of the HINS, an 8 GeV superconducting proton linac [1] [2]. The front end section operates at 325 MHz and uses a mixture of normal-conducting and superconducting devices. Initial acceleration of the beam is achieved by a Radio Frequency Quadrupole (RFQ) from 0.05 MeV to 2.5 MeV and Room Temperature Crossbar H-type (RTCH) accelerating cavities up to 10 MeV [3][4]. Three types of superconducting resonators accelerate the beam from 10 MeV to 400 MeV: Single Spoke Resonators type-1 (SSR1), Single Spoke Resonators type-2 (SSR2) and Triple Spoke Resonators (TSR) [6][7].

An earlier paper [Pac07] described the fabrication and frequency tuning of the SSR1-01, the first SSR1 prototype. This paper continues with descriptions of the chemical polishing, the high pressure rinse, and the initial high-gradient cold tests of SSR1-01, as well as some aspects of the fabrication and tuning of the second prototype, SSR1-02.

II. RF DESIGN OF SINGLE SPOKE RESONATORS

The main criteria of the cavity RF design are to minimize the peak surface electric and magnetic field ratios, E_{peak}/E_{acc} and B_{peak}/E_{acc}, where E_{acc} is the accelerating gradient.

The optimization of the shape of SSR1 was performed using MWS software and described in [6].

Table 1 shows the RF parameters of the optimized SSR1. The effective length used to define E_{acc} is equal to $\beta\lambda$.

TABLE 1 MAIN PARAMETERS OF SSR1

Operating temperature	4.4 K
Accelerating gradient	10 MV/m
Quality factor at operating gradient	$>0.5 \times 10^{-9}$
Beam Pipe ID	30 mm
Lorentz force detuning coefficient	3.8 Hz/(MV/m)^2
E_{peak}/E_{acc}	3.86
B_{peak}/E_{acc}	6.25 mT/(MV/m)
G	84 Ω
R/Q_0	242 Ω
Geometrical Beta	0.21

III. FABRICATION

The first SSR1 resonator, SSR1-01, was fabricated by E. Zanon [10] and is currently undergoing cold tests at Fermilab. SSR1-02 was manufactured by C.F. Roark Welding & Engineering Co., Inc. [11] and was completed in July, 2008. Two more resonators are currently being fabricated at IUAC in New Delhi [12].

Figure 1 The completed SSR1-02 Resonator.

The resonator is fabricated from high RRR niobium sheets with a nominal thickness of 3.15 mm that is reduced by forming and BCP to an average of 2.8 mm. Three sets of stiffeners (daisy ribs, donut ribs and circumferential ribs), all having a stock thickness of 6.35 mm and made of reactor-grade niobium, are welded on the outside of the cavity. The two beam flanges, the vacuum flange and the power coupler flange of the resonator are made of 316L stainless steel and are joined to the niobium cavity by brazing. This cryogenic leak-tight copper-brazed transition was developed at Argonne National Laboratory (ANL) and described in [8].

Manuscript received -- August 2008. (Write the date on which you submitted your paper for review.) This work was supported by the U.S. Department of Energy under contract number DE-AC02-76CH03000.

Authors are with the Fermi National Accelerator Laboratory (FNAL), Batavia IL 60510.

† Phone: +1 630-840-4401; fax +1 630-840-8036; e-mail: leoristo@fnal.gov.

The fabrication of SSR1-02 was substantially similar to the fabrication of SSR1-01 except for a few items. Each end wall was formed from a single piece in contrast to two pieces joined by Electron Beam (EB) welding. Weld beads on the interior (RF) surface were left intact instead of being ground even with the surface when accessible.

Once the three major sub-assemblies were completed, trimming and final welding operations were performed to complete the resonator.

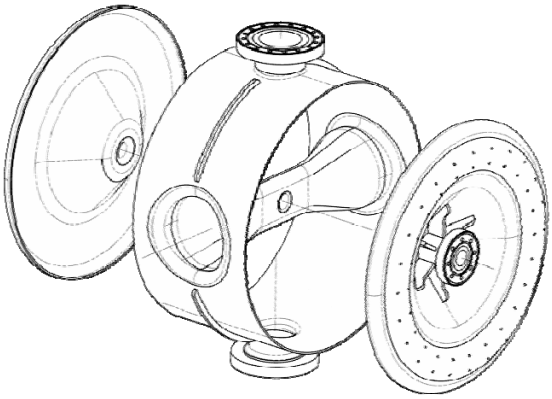

Figure 2 Exploded view of the SSR1 resonator showing the three major sub-assemblies.

A. *Trimming operations*

Initially the shell assembly was installed on a vertical lathe and material was removed on both sides until a continuous cut was established. This was done to obtain a satisfactory surface flatness on the weld joint. The three sub-assemblies were then clamped together in a dry fit to measure the resonant frequency. Measuring and machining steps were repeated until the frequency of 325.389 MHz was reached. As described in [9], the target frequency that was set for SSR1-01 for the trimming operations was 324.535 MHz. With the intent of keeping the two gaps of SSR1-02 within tolerance, we opted for less trimming in favor of a yet to be performed inelastic deformation, as the latter has a higher tuning sensitivity. The average sensitivity of the resonant frequency to trimming recorded was 376 kHz/mm.

B. *Final welding operations*

Before the final welding of the two end wall assemblies to the shell assembly, the parts were measured on a coordinate measuring machine to record length and roundness. To ensure a step on the weld joint not greater than 0.5 mm, the welding fixture was designed with set screws, protected with niobium shims, around the perimeter.

Before welding, the pressure in the EB welding chamber was always less than or equal to 30 μTorr. Twelve, 2.5 cm long tack welds were equally spaced around the perimeter. The penetration of the tack weld is about 50%. After cool down and venting, the fixture was removed to make space for the continuous welds. The seal weld pass and the final weld pass took 10 minutes each at 15 cm/min. After 1 hour in vacuum and 40 minutes in argon, surface temperatures when the chamber was opened were in the range of 45-60 ºC. After visual inspection and recording of the weld shrinkage, the same procedure was followed to weld the second end wall. The whole welding procedure will be expedited by performing more welds during the same pump down in the future once more weld shrinkage and frequency shift data is available.

IV. Buffered Chemical Polishing

The Fermilab Vertical Test Stand (VTS), a liquid helium Dewar designed for high-gradient testing of bare 9-cell ILC cavities, was used for the first cold test of the bare SSR1-01. The interior surface of the cavity first had to be prepared for high-gradient testing. The SSR1-01 was immersed in a bath of Ultra-Pure Water (UPW) with a degreasing agent and ultrasonically cleaned. It was then taken to the ANL G150 facility for Buffered Chemical Polishing (BCP) followed by a High Pressure Rinse (HPR).

The BCP used the standard acid mixture of HF (48%), HNO_3 (69.5%) and H_3PO_4 (85%) in the volume ratio 1:1:2, respectively. During BCP, acid flow and temperature were controlled in the following manner. The cavity was immersed in a bath of UPW that was initially cooled to 7.5 ºC by a continuously operating chiller. The cavity interior, sealed from the water bath, was connected to a pump for acid circulation. The cavity was oriented with the power coupler port and the vacuum port along the vertical axis and the beam pipes along the horizontal axis. In order to begin etching, acid (earlier chilled to 14 ºC) was pumped up through the bottom port to fill the interior of the cavity plus an "overflow bucket" connected to the top port. After shutting off the source of acid, the closed loop circulation pump drew acid from the overflow bucket and sent it back to the cavity through flanges on both beam pipes. Heat generated by the etching was dissipated through the cavity walls (including the spoke walls) to the continuously cooled water bath. Both the acid and water-bath temperatures were monitored during the etching.

In order to obtain a total etching of ~120 μm and keep the niobium content in the acid below 10 g/l, the spent acid was replaced with fresh acid about half way through the etching. Given the asymmetry in the acid flow pattern, the cavity was flipped top to bottom between the two etching sessions. The reduction in wall thickness was monitored at 20 locations (mostly at high E or B surface fields) using an ultrasonic thickness gauge.

The wall thickness reduction averaged 52 μm after the first 70 minute session and 119 μm after the flipping the cavity and etching another 90 minutes. The acid temperature averaged 15.9 ºC and ranged between 14.9 ºC and 17.0 ºC during the etching. The thickness reduction was not as uniform as hoped, with both the thickness gauge measurements and resonant frequency shift indicating up to a factor of two more etching near the beam pipe (high E) than near the shell (high B). Also, the smallest thickness reductions were measured near the power coupler port and vacuum port, where one may expect reduced etching due to spent acid when at the bottom and due to gas pockets when at the top. We have plans to distribute the acid flow more uniformly in the future.

V. High Pressure Rinse

After BCP, the SSR1-01 was moved from the chemistry hood to the class 10 clean area for HPR. The G150 UPW distribution consists of a long wand with a nozzle at the end that produces six water jets, two each at +45º, 90º, and -45º to the wand axis. The wand rapidly rotates about the axis and travels along the axis (into or out of the cavity) at ~3 cm/min. In order for a jet to directly spray on all the interior cavity surfaces, including ports and beam pipes, the orientation of the SSR1 was changed six times with the HPR lasting ~20 minutes at each orientation. After completing the HPR, the cavity was left in a good orientation for drainage (vacuum port up) and left to dry in the class 10 clean area overnight. Blank-off flanges were installed the next day, and the cavity was taken to the class 10 clean room in the MP9 building at Fermilab for final preparations before testing in the VTS.

VI. High Gradient Measurements

A fixed-length power coupler antenna with $Q_{ext} = 5.9x10^8$ was installed at one beam pipe flange, and a fixed-length transmitted power antenna with $Q_{ext} = 3.5x10^{10}$ was installed at the other beam pipe flange. The SSR1-01 was mounted in the VTS Dewar with the power coupler port up and the beam pipe along the horizontal axis.

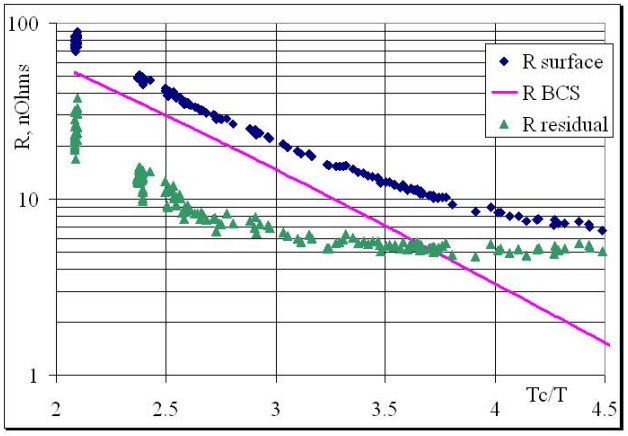

Figure 3 Surface resistance of the cavity during cool down allows the calculation of residual surface resistance.

There have been three test sessions in the VTS; Test 1 in February, 2008, Test 2 in March, 2008 and Test 3 in July, 2008. For Test 1 (the first cold test of the cavity) and Test 2, the VTS did not yet have a cavity vacuum system, so the SSR1 was evacuated (to $2x10^{-6}$ Torr for Test 1) and sealed before installation into the Dewar. In Test 1, Q_0 was measured as a function of temperature, T, as the temperature was lowered from 4 ºK to 2 ºK at $E_{acc} = 2$ MV/m. As shown in Figure 3, this data was used to obtain the surface resistance, $R_s(T) = R_0 + R_{BCS}(T)$ with a fit residual resistance of $R_0 = 5.1$ nΩ.

In both Tests 1 and 2, the resonant frequency was measured as a function of the liquid helium bath pressure, shown in Figure 4, and as a function of E_{acc}^2, shown in Figure 5. The measured pressure sensitivity agrees quite well with the value of -630 Hz/Torr predicted by the MWS-ANSYS [13][14] simulation of the bare cavity (the simulation predicts a much smaller value of -30 Hz/Torr when the helium vessel is attached).

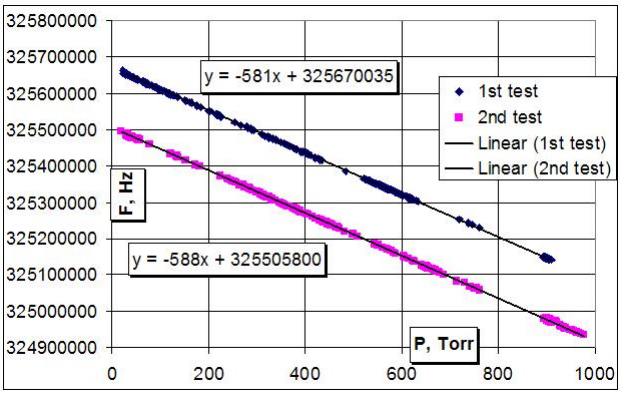

Figure 4 Bare cavity resonance frequency sensitivity to helium bath pressure.

The measured Lorentz force detuning coefficient of ~-4 $Hz/(MV/m)^2$ (Figure 5) agrees much better with the simulation's prediction of the cavity with the helium vessel attached, -3.8 $Hz/(MV/m)^2$, than bare, -13.4 $Hz/(MV/m)^2$. This is not yet understood.

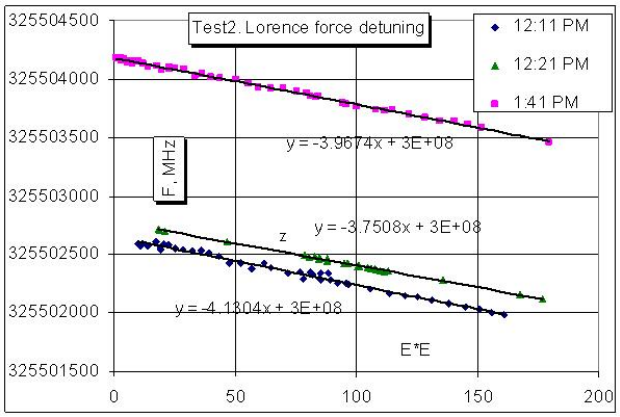

Figure 5 Lorentz force detuning. Frequency vs. accelerating gradient squared.

When increasing E_{acc} at 2 ºK in Test 1, several multipacting barriers were encountered and we could not process beyond one at ~6 MV/m. During Test 1, the SSR1-01 was instrumented with RTD temperature monitors on the shell, around most of the circumference at the endwalls and around the ends of the spoke. The temperature monitors indicated that the multipacting occurred only at the bottom of the cavity near the vacuum port. In addition, X-ray detecting diodes were mounted in the liquid helium just beyond the beam pipe flanges and "off axis" at about a 30º angle to the flanges. The relative intensity of detected X-rays during the multipacting at 6 MV/m indicated that some electrons from the multipacting migrated up to the accelerating gap, and the accelerated electrons interacted with a beam pipe flange to produce the X-rays.

After ending Test 1 and warming to room temperature, the cavity vacuum was measured to be $1.5x10^{-3}$ Torr, 1 to 2 orders of magnitude higher than expected if the cavity was just sitting on the shelf. An RGA indicated that the cavity contained water and hydrogen, but no detectable helium. The poor

vacuum and evidence for multipacting predominately on the bottom indicated a possible problem with condensates forming during both the cool down and the multipacting. It was decided to immediately try a second test if a better initial vacuum could be obtained.

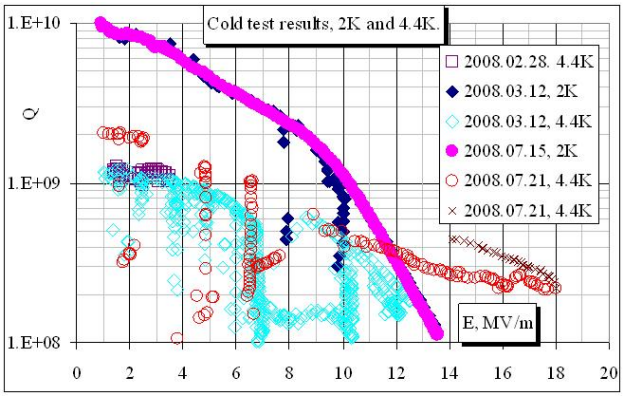

Figure 6 Quality factor of the cavity .vs. accelerating gradient. Data labeled 2008.02 are from Test 1, 2008.03 from Test2, and 2008.07 from Test 3. The X's are from the backward scan noted in the text.

Test 2 began with a cavity vacuum of 1.2×10^{-7} Torr (again there was no active pumping in the VTS). The E_{acc} scan of Q_0 at 2ºK, shown in Figure 6, reached 13.5 MV/m before field emission prevented further increase with our 200 W power supply. The multipacting barriers shown in the figure were also encountered upon subsequent E_{acc} scans in Test 2.

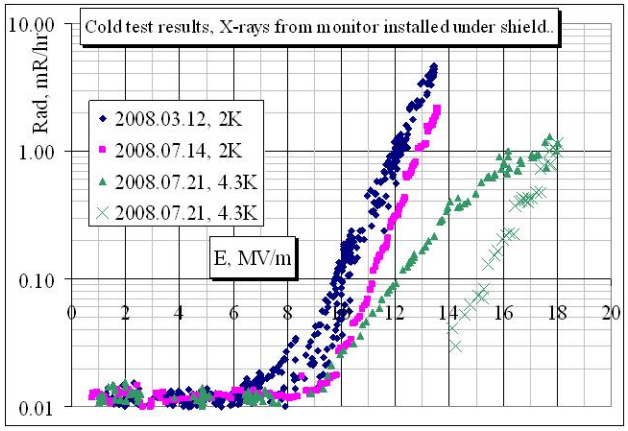

Figure 7 X-ray intensity .vs. accelerating gradient. The data labeled 2008.03 are from Test 2, and 2008.07 from Test 3. The X's are from the backward scan noted in the text.

Figure 7 shows the X-ray intensity from a detector installed just under the VTS Dewar's top plate. Field emission clearly became a significant power drain above ~8 MV/m in Test 2. An E_{acc} scan of Q_0 at 4.4ºK, shown in Figure 6, ended with a thermal quench at 12.5 MV/m. Following the warm-up after Test 2, the vacuum was measured to be 5.9×10^{-4} Torr and the RGA again detected only hydrogen and water. As noted earlier, the larger than expected degradation in vacuum may be partly due to interstitial gasses released during multipacting.

With the presence of field emission at high E_{acc}, we hoped to do an improved HPR before the next VTS test, but the VTS scheduling allowed for a third test before another HPR could be arranged at ANL. Steps were taken to optimize the cavity vacuum throughout Test 3. A two day long 120 ºC vacuum bake of the SSR1-01 was performed shortly before the cavity was installed in the VTS. In addition, the newly commissioned cavity vacuum system of the VTS, which allows a vacuum at the cavity of $\sim 8 \times 10^{-8}$ Torr, was used during the test.

Test 3 started with an E_{acc} scan of Q_0 at 2ºK, and the result, shown in Figure 6, was essentially identical to that from Test 2, with the important exception that after the initial scan, the cavity no longer fell into multipacting barriers near the operating gradient of 10 MV/m when raising the field. The VTS was left to warm to ~3.5ºK overnight, and the following morning E_{acc} could not be raised above 15 kV/m, indicating a helium leak. After warming up to room temperature, helium was clearly seen in an RGA, but efforts to isolate the source of the leak at that time were unsuccessful.

After cooling back down to 4.4ºK , the field could again be raised, and the E_{acc} scan of Q_0 shown in Figure 6 was taken. In this case, data taken during the initial increase in field (including processing multipacting barriers) and data subsequently taken working backward from the maximum field are plotted with different symbols.

There are several interesting features of this scan. Q_0 at low E_{acc} is nearly a factor of two higher than that recorded in the 4.4 ºK scans in Tests 1 and 2. This corresponds to a reduction in surface resistance from 70 nΩ to 45 nΩ, and we believe this may be due to the 120 ºC bake. Note that an improvement was observed only in $R_s(4.4K)$, but not in $R_s(2K) \approx R_0$.

Up to 10 MV/m, the cavity behaved similarly to Test 2, but after 10 MV/m, the cavity properties started changing. The intensity of X-rays dropped (figure 7) and Q_0 increased (figure 6). It appears that helium processing of field emitters had occurred, allowing E_{acc} to reach 18 MV/m, well beyond the earlier maxima of 12.5 MV/m at 4.4°K and 13.6 MV/m at 2°K. This scan could have continued to higher field levels, since power was not yet limited by field emission.

A backward scan in field was started to record any change in Q_0 after the initial processing. As evidenced by the reduced X-ray intensity, shown in Figure 7, field emission was considerably lower in the backward scan with a corresponding increase in Q_0, shown in figure 6. After recording the data point at 14 MV/m, the cavity again became inoperable (the field could not be raised past 20 kV/m) indicating further problems with the helium leak. Test 3 ended, and the leak was eventually isolated to the RF feed through for the power coupler antenna. The helium leak was probably a two-edged sword, sometimes not allowing operation (possibly due to increased multipacting), but also allowing the processing of field emitters to achieve higher fields.

VII. ACKNOWLEDGEMENTS

The authors wish to acknowledge the efforts of S. Gerbick, M. Kedzie, and M. Kelly of ANL; T. Arkan, D. Arnold, D. Assell, G. Romanov, and B. Smith of Fermilab; and T. Roark and D. Osha of Roark.

REFERENCES

[1] G. W. Foster and J. A. MacLachlan, "A Multi-Mission 8 GeV Injector Linac as a Fermilab Booster replacement", Proc. of the LINAC-2002, Gyeongju, Korea.

[2] P.N. Ostroumov et al, "Front End Design of a Multi-GeV H-Minus Linac", Proc. Of the PAC-2005, Knoxville, Tennessee, May 2005.

[3] L. Ristori, G. Romanov, T. Khabiboulline et al., "Design of normal conducting 325 MHz crossbar h-type resonators at Fermilab", LINAC-2006, Knoxville, Tennessee, August 2006.

[4] L. Ristori, G. Romanov, T. Khabiboulline et al., "Fabrication and test of the first normal-conducting crossbar h-type accelerating cavity at Fermilab for HINS", Proc. of the PAC-2007, Albuquerque, New Mexico.

[5] T. M. Page, et al., "High Intensity Neutrino Source Superconducting Solenoid Cryostat Design", presented at CEC, Chattanooga, TN, 2007.

[6] G. Apollinari, I. Gonin, T. Khabiboulline, G. Lanfranco, G. Romanov, "design of 325 MHz Single Spoke Resonator at FNAL", Proc. Of the 12th International Workshop on RF Superconductivity, Cornell University, Ithaca, New York, July 2005.

[7] G. Apollinari, I. Gonin, T. Khabiboulline, G. Lanfranco, F. McConologue, G. Romanov, "Design of 325 MHz Single and Triple Spoke Resonators at FNAL", Proc. of the LINAC-2006, Knoxville, Tennessee, August 2006.

[8] J. D. Fuerst et al., "Niobium to stainless steel braze transition development", Proc. of the 11th workshop on RF-superconductivity, SRF 2003, DESY, September 2003.

[9] G. Lanfranco et al., "Production of 325 MHz single spoke resonators at FNAL", Proc. of PAC07, Albuquerque, New Mexico, USA.

[10] Ettore Zanon Spa - Via Vicenza 113 - 36015 Schio (Vi) Italy – www.zanon.com.

[11] C.F. Roark Welding & Engineering Co, Inc. - 136 N. Green St. - Brownsburg, IN 46112, USA – www.roarkfab.com.

[12] Inter University Accelerator Centre, Aruna Asaf Ali Marg – P.O. Box 10502, New Delhi – 110067, India - www.iuac.ernet.in.

[13] CST MICROWAVE STUDIO® (CST MWS), www.cst.com.

[14] ANSYS Multiphysics™ of Ansys Inc., www.ansys.com.